



## Original Research Article

### Synthesis and Characterization of Cordierite Ceramics with varying Amounts of Alumina and Magnesia

Mgbemere, H.E., Obidiegwu, E.O. and \*Moka, N.N.

Department of Metallurgical and Materials Engineering, Faculty of Engineering, University of Lagos, Akoka, Lagos State, Nigeria.

\*ngozimoka@gmail.com; hmgbemere@unilag.edu.ng

<http://doi.org/10.5281/zenodo.5805171>

#### ARTICLE INFORMATION

##### Article history:

Received 24 Sep, 2021

Revised 01 Nov, 2021

Accepted 16 Nov 2021

Available online 30 Dec 2021

##### Keywords:

Cordierite

Silica

Magnesia

Alumina

Solid-state

Sintering

Diesel particulate filter

#### ABSTRACT

*Cordierite is a naturally occurring mineral with unique characteristics and can be synthesized from locally available raw materials. One of the well-known applications for this material is in diesel particulate filter (DPF) which helps to reduce the pollution rate from automobiles. The rate of pollution in Nigeria is very high partly due to the low availability of filters. In this work, cordierite was produced using alumina, magnesia and silica by varying the amounts of alumina and magnesia. Solid-state synthesis method was used while characterization tools like X-ray diffraction (XRD), X-ray fluorescence (XRF), scanning electron microscope (SEM), bulk density, and differential thermal analysis (DTA) were used in the analysis. The chemical analysis showed that 77.64%  $Al_2O_3$ , 76.7%  $MgO$  and 94.97% of  $SiO_2$  were obtained from the raw materials respectively. The phase analysis showed that as the  $MgO$  content increased, the intensity of the peaks at  $44^\circ$  and  $60^\circ$  increased and the enstatite phase was formed. Both endothermic and exothermic peaks were observed from thermal studies. The sample morphologies indicated that increasing  $MgO$  content led to a reduction in the average grain size of the particles. The results indicate that while cordierite formation commenced, complete densification was not attained possibly due to the lower sintering temperature used.*

© 2021 RJEES. All rights reserved.

## 1. INTRODUCTION

Air pollution is a notable cause of illness, social phobia, and death globally. It is particularly severe in Nigeria; the country with the highest number of premature deaths due to ambient particulate matter pollution in sub Saharan African region (Croitoru *et al.*, 2020). It is especially worrying in Lagos, the country's commercial capital and one of the world's most populated cities. Despite growing concerns about its deadly

impacts, there is currently no reliable monetary estimate of the effects of ambient air pollution, or a comprehensive control plan in Lagos (Croitoru *et al.*, 2020). Using available ground-level monitored data and the most recent valuation techniques, it was estimated that in 2018 alone, ambient fine particulate matter (PM<sub>2.5</sub>) caused about 11,200 premature deaths, and generated a health cost of approximately \$2.1 billion in Lagos. This amount is equivalent to about 2.1 % of Lagos' GDP in the same year. These observations call for an urgent plan of action to improve air quality in the city, with a primary focus on the main pollution sources: road transport, industrial emissions, and power generators (Croitoru *et al.*, 2020).

Cordierite is a magnesium aluminum silicate mineral with the chemical formula  $2\text{Al}_2\text{O}_3 \cdot 2\text{MgO} \cdot 5\text{SiO}_2$ . It is an important naturally occurring ceramic material that has gained considerable interest for a broad range of industrial applications due to its excellent properties (Gonzalez-Velasco *et al.*, 1999). Its unique characteristics such as its high mechanical strength, high chemical durability, low dielectric constant, and low coefficient of thermal expansion (CTE) make it an interesting candidate for many industrial applications, such as monolithic catalyst support (Gonzalez-Velasco *et al.*, 1999). One of the most common applications of cordierite is as ceramic monolithic support (Gokce *et al.*, 2004).

Monolithic catalyst supports are used as diesel particulate filters (DPF), catalytic incineration, catalyst support for chemical processes, and vehicle emissions control. Cordierite is the most common ceramic wall-flow filter used for diesel particulate filters as it filters out a very high percentage of carbon particles and is fairly cheap. DPF is an exhaust after-treatment device that traps particulate matter such as soot and ash from exhaust gas or diesel engine. It offers a more excellent way to reduce emissions in the transportation and industrial sector. It is therefore useful and effective as honeycomb-shaped catalyst carriers in automobile exhaust systems, as a radiator for gas turbines, as plating material for circuit boards (Zhu *et al.*, (2012).

Porous cordierite ceramic honeycombs are currently being considered as one of the leading candidates for oxidizing and trapping the carbonaceous particulate emissions from automobiles (Gonzalez-Velasco *et al.*, 1999). For some years now, porous ceramic substrates have been used as automobile catalyst supports to help facilitate the conversion of carbon monoxide (CO) and hydrocarbon (HC) emissions to carbon dioxide (CO<sub>2</sub>) and water (H<sub>2</sub>O) by a redox reaction (Mai *et al.*, 2015).

Cordierite has to be synthesized from natural raw materials or synthetic powders having high purity and which are readily available because the natural mineral is not abundant or pure enough (Gonzalez-Velasco *et al.*, 1999). Alhilil *et al.* (2013) characterized cordierite-mullite ceramics produced from natural raw materials. They concluded that a minimum addition of pure boehmite to magnesite, quartz, and natural kaolin, can be used to produce ceramics with different cordierite-mullite ratios. Cao *et al.* (2016) and Gonzalez-Velasco *et al.* (1999) conducted researches to gain a better understanding of some of the processes involved in the preparation of cordierite monolithic honeycomb substrates by solid-state reaction. They deduced that to manufacture cordierite with improved crystallinity, the particle size of the starting raw materials should be carefully controlled. El-Buaishi *et al.* (2012) as well as Naskar and Chatterjee (2004) considered the reduction in the cost of producing cordierite and stated that the cost of preparation will be reduced and the process made more environmentally friendly by using natural raw materials via sol-gel preparation method. Some other researchers studied the low-temperature synthesis of the cordierite phase in ceramic mixtures of natural raw materials using boron oxide (B<sub>2</sub>O<sub>3</sub>) as an additive to reduce the formation temperatures. Under mechanical activation, the synthesis of cordierite was achieved and it was concluded that economically, the use of naturally occurring raw materials is the best option (Khabas *et al.*, 2003; Sumi *et al.*, 2004 and Gunay 2010). From the literature reviewed, the effect of varying the amounts of Alumina and Magnesia has not been very well investigated.

This research aims to determine the possibility of using locally available raw materials to synthesize cordierites as well as to investigate the effect of varying the amounts of alumina and magnesia on the properties of cordierite ceramics. The study covers the formation of cordierite via solid-state sintering process using magnesia, silica, alumina, and starch as a binder.

## 2. MATERIALS AND METHODS

### 2.1. Material Collection

The raw materials used are alumina ( $\text{Al}_2\text{O}_3$ ), silica ( $\text{SiO}_2$ ), magnesia ( $\text{MgO}$ ), and starch. They were procured from the Ojota chemical market in Lagos, Nigeria.

### 2.2. Sample Preparation

The formulation of the samples used in this research were labeled as A, B, C, D, and E as shown in Table 1. Composition A contains the stoichiometric composition of cordierite while samples B to E had the  $\text{Al}_2\text{O}_3$  amounts slightly reduced while that of  $\text{MgO}$  was increased by the same weight percent. The Table also shows the amounts of the raw powders used for the synthesis.

Table 1: Composition (wt. %) of oxide raw materials used in the synthesis of Cordierite

Samples	Composition	Wt. (%)		
		$\text{Al}_2\text{O}_3$	$\text{MgO}$	$\text{SiO}_2$
A	$2\text{Al}_2\text{O}_3\cdot 2\text{MgO}\cdot 5\text{SiO}_2$	34.9	13.7	51.4
B	$1.75\text{Al}_2\text{O}_3\cdot 2.25\text{MgO}\cdot 5\text{SiO}_2$	31.4	15.8	52.8
C	$1.5\text{Al}_2\text{O}_3\cdot 2.5\text{MgO}\cdot 5\text{SiO}_2$	27.7	18.1	54.2
D	$1.25\text{Al}_2\text{O}_3\cdot 2.75\text{MgO}\cdot 5\text{SiO}_2$	23.7	20.5	55.8
E	$\text{Al}_2\text{O}_3\cdot 3\text{MgO}\cdot 5\text{SiO}_2$	19.5	23.0	57.5

The raw powders ( $\text{Al}_2\text{O}_3$ ,  $\text{MgO}$  and  $\text{SiO}_2$ ) were first placed in a ball mill for size reduction and milled separately for 48 hours to obtain powders that are adequately fine-grained to be mixed homogeneously. They were then sieved using a mesh of sieve size  $125\ \mu\text{m}$  and weighed carefully using a digital weighing balance to obtain the composition of each sample. The weighed-out compositions for each raw material was then ball-milled again for 12 hours to achieve proper homogeneity of the mixed oxide powder. A smooth paste was formed by mixing 5 g of powdered starch, 20 g of deionized water, and 40 g of the mixed  $\text{Al}_2\text{O}_3$ ,  $\text{MgO}$  and  $\text{SiO}_2$  powders. A cylindrical metallic mould used for pressing was then lubricated with vegetable oil while the powder compaction was done using a hydraulic press. The pressed sample was gently removed after the compaction and dried for 5 days in the air and sintered using a kiln. The sintering process began with slow-controlled heating to prevent the compacted body from breaking while the starch was being removed. The temperature was then increased gradually till it got to a temperature of  $1200\ ^\circ\text{C}$  where it was held for 2 hours at a heating and cooling rate of  $10\ ^\circ\text{C}/\text{min}$ .

### 2.3. Sample Characterization

#### 2.3.1. X-ray diffraction and X-ray fluorescence analysis

The XRD patterns of the samples were determined at the National Geosciences Research Laboratories (NGRL) Kaduna. It was done using an EMPYREAN diffractometer system operated with Cu anode and K-alpha radiation (K-Alpha1 wavelength:  $1.540598\ \text{\AA}$ , K-alpha 2 wavelength:  $1.544426$ ). The operating tube current was 40 mA and the generator voltage of 45 kV. The scanning range was from  $5.0024^\circ$  to  $74.9684^\circ$  with a scan step size of  $0.0262602^\circ$ . The chemical compositions of the starting materials were obtained using an XRF analyzer.

#### 2.3.2. Differential thermal analysis

The differential thermal analysis was carried out with a thermogravimetric analyzer (TGA) (PerkinElmer TGA 4000, Netherlands). The maximum operating temperature used is  $900\ ^\circ\text{C}$  while the heating rate of  $20\ ^\circ\text{C}/\text{min}$  was used.

### 2.3.3. Scanning electron microscopy

The morphology of the sintered samples was observed using a scanning electron microscope at the National Geosciences Research Laboratories Kaduna. It was operated at a voltage of 15 kV. First, a sample stub with a double adhesive was first placed and, thereafter the sample was placed on it. It was then taken to a sputter coater (Quorum-Q150R plus E) with 5 nm of gold. It was then placed on a charge reduction sample holder and introduced into the column of the SEM machine (Phenom ProX, Phenomworld Eindhoven Netherlands) where it was viewed from a NavCam before it was sent to SEM mode with different magnifications.

### 2.3.4. Bulk density

The bulk density was calculated using Archimedes' principle. The sintered samples were first weighed to determine their dry weight. It was then recorded and repeated thrice for each sample to increase the accuracy of the results. Each sample was then immersed in a 250 ml measuring cylinder filled with deionized water up to 200 ml level. The volume of the water displaced was recorded after five minutes intervals for three consecutive times. Bubbles were observed as the samples were immersed in water through the pores. The volume average of the three displacements was then calculated and subtracted from the initial water volume ( $V_w = 200$  ml) to get the volume of the sample in water ( $V_o$ ). The bulk densities of the samples were calculated using the Archimedes principle of upthrust using Equation 1. A picture of the sintered samples is shown in Figure 1.

$$\text{Density} = \frac{\text{mass of sample (g)}}{\text{Volume of water displaced (V}_o\text{)}} \quad (1)$$

$$V_o = V_1 - V_w \quad (2)$$

Where  $V_o$  = volume of the sample in water,  $V_1$  = volume of water + sample, and  $V_w$  = volume of water



Figure 1: Cordierite samples numbered A to E sintered at 1200 °C for 2 hours

## 3. RESULTS AND DISCUSSION

### 3.1. XRF Analysis

The chemical compositions of the starting materials were obtained using XRF analyzer are given in Table 2. The results indicate that the starting materials contain  $\text{Al}_2\text{O}_3$ ,  $\text{SiO}_2$ , and  $\text{MgO}$  as the major constituents with some minor constituents as impurities. These compounds ( $\text{Al}_2\text{O}_3$ ,  $\text{MgO}$  and  $\text{SiO}_2$ ) are necessary for the formation of cordierite (Gunay 2010). The alumina sample was found to contain only 77.64%  $\text{Al}_2\text{O}_3$  and the rest are impurities. The magnesia also contains 76.7% of  $\text{MgO}$  while the silica contains 94.97% of  $\text{SiO}_2$ . These results are similar to the results obtained by Eing *et al.* (2016). A preliminary investigation of the composition of sample A showed that the  $\text{SiO}_2$  content is 48.79%,  $\text{Al}_2\text{O}_3$  content is 33.12% and  $\text{MgO}$  content is 13.09%.

Table 2: Chemical composition of alumina, silica, magnesia in wt. %

Compound	Alumina (wt %)	Magnesia (wt. %)	Silica (wt. %)
Fe <sub>2</sub> O <sub>3</sub>	0.03	0.31	0.09
Na <sub>2</sub> O	0.40	0.29	1.61
MgO	0.66	76.70	0.60
Al <sub>2</sub> O <sub>3</sub>	77.64	1.65	1.06
SiO <sub>2</sub>	1.14	0.18	94.97
P <sub>2</sub> O <sub>5</sub>	0.00	0.02	0.76
SO <sub>2</sub>	0.04	0.10	0.52
CaO	0.02	0.83	0.03

### 3.2. XRD Analysis

The XRD results indicate that the major crystalline phase present in samples A, B, C, and D was enstatite while enstatite and forsterite are present in sample E. This shows that in sample E, the structural water is released when the bonds are broken and the increase in MgO content facilitated the precipitation of forsterite (Zhu *et al.*, 2012). This is similar to the result obtained by Eing *et al.* (2016). It can be observed in Figure 2 that the peak intensity at  $2\theta = 23^\circ$  decreased as the magnesia content increased but with further increase in  $2\theta = 43^\circ$  and  $62^\circ$  the peak intensity increased with increase in magnesia content. This corresponds to the result obtained by Zhu *et al.* (2012). There is however no clear trend on how the increasing MgO and decreasing Al<sub>2</sub>O<sub>3</sub> amounts affected the cordierite ceramics.

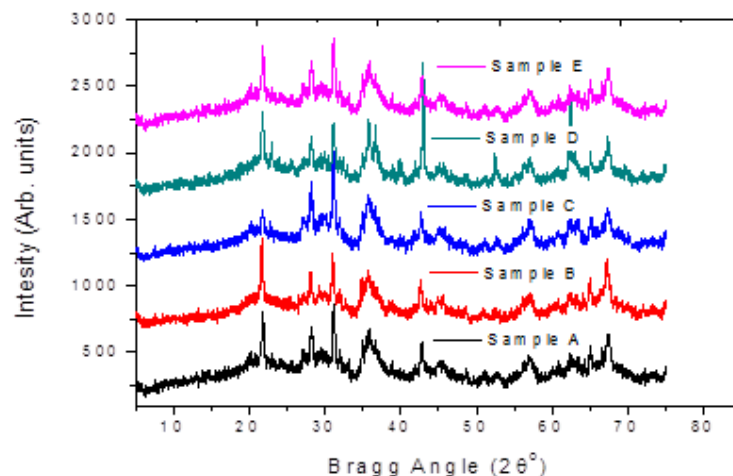


Figure 1: X-ray diffraction patterns of the sintered cordierite samples A to E

### 3.3. DTA Analysis

The thermal analysis results of the cordierite samples A to E using the differential thermal analyser are shown in Figure 3. It can be observed that for all the samples, there was one major endothermic peak which occurred at temperatures ranging from 320 °C and 450 °C. A small endothermic peak was also observed at temperatures between 100 °C and 200 °C corresponding to the loss of surface absorbed water. The major endothermic peaks in the samples can be attributed to the loss or release of the chemically bound water (Zhu *et al.*, 2012). The endothermic peak in Sample A took place at 338 °C and is the sharpest. As the amount of MgO increases and Al<sub>2</sub>O<sub>3</sub> decreases, the temperature of the endothermic peak shifts while the intensity also reduces. The endothermic peak in Sample B occurred at 383 °C while that of sample C was at 390 °C. The endothermic peaks for samples D and E occurred at 388 °C signifying that at this point, increasing the MgO content while

decreasing the  $\text{Al}_2\text{O}_3$  content did not have any significant effect. From a temperature of  $488\text{ }^\circ\text{C}$ , the formation of the endothermic peaks in the samples ended. From this temperature to  $900\text{ }^\circ\text{C}$ , where the experiment was terminated, a flat plateau was maintained. This indicates that irrespective of the composition, above  $488\text{ }^\circ\text{C}$ , the samples become stable such that there are little or no reactions taking place.

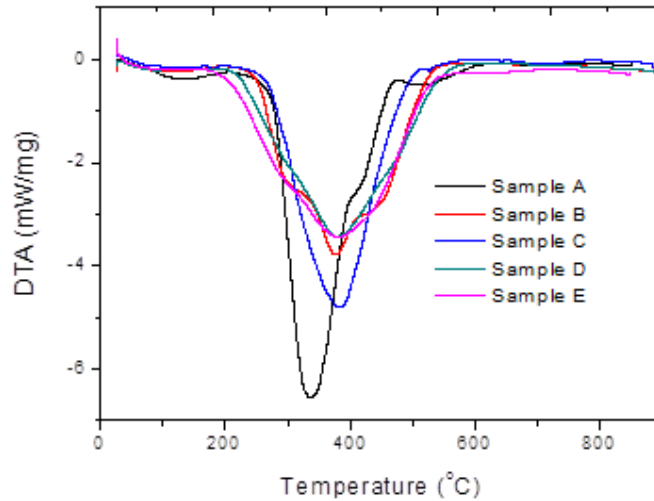
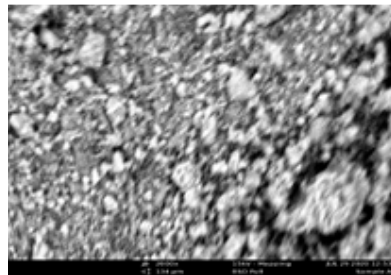


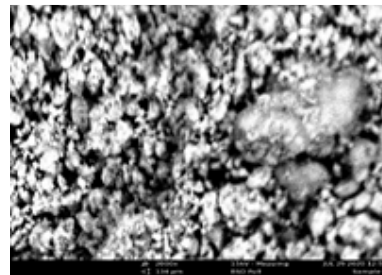
Figure 3: A graph of derivative weight as a function of temperature for samples A to E

### 3.4. SEM Analysis

The morphology of the samples A to E at various magnifications is shown in Figure 4. The micrographs show that as the amount of MgO increased while the  $\text{Al}_2\text{O}_3$  decreased, the average grain size of the samples slightly decreased. The grains also gradually become uniform with increasing MgO content because a few large grains could be observed in both samples A and B only. The typical sintering temperature for cordierite is approximately  $1350\text{ }^\circ\text{C}$  but the samples in this study were sintered at  $1200\text{ }^\circ\text{C}$ . It can also be observed that the pore sizes and the distribution of the pores are not uniform for all the samples. The heterogeneous nature of samples A and B could be due to the low sintering temperature used. It is possible that because of this temperature, complete diffusion of the species did not take place similar to what has been reported by Ning *et al.* (2018).



(a)



(b)

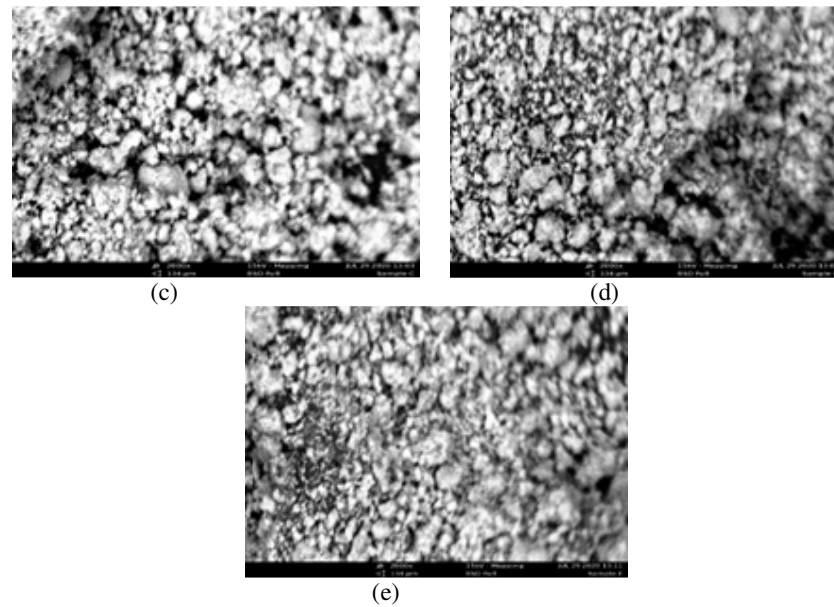


Figure 4: Scanning electron microscope images of sintered cordierite samples A to E

### 3.5. Bulk Density

The bulk density values for the samples are shown in Figure 5. Sample A has the highest density value of  $2.25 \text{ g/cm}^3$ . The bulk density result for the other samples shows a slight fluctuation in the values as the composition of MgO increases while that of  $\text{Al}_2\text{O}_3$  decreases. A possible reason for this could be that the samples required a slightly higher temperature for sintering compared to that actually used. This is similar to the result obtained by Jianfeng *et al.* (2018). The density values for the samples ranged from  $1.95 \text{ g/cm}^3$  to  $2.1 \text{ g/cm}^3$ .

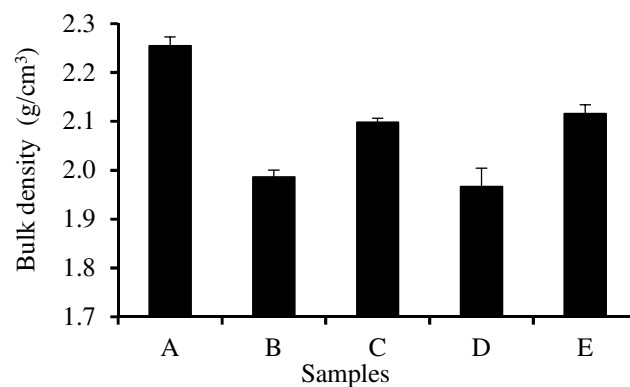


Figure 5: Bulk density values for the cordierite samples A to E

## 4. CONCLUSION

Cordierites with varying amounts of  $\text{Al}_2\text{O}_3$  and MgO have been synthesized and characterized in this research. The preliminary chemical composition analysis on the cordierite indicates that it contains 48.79% of  $\text{SiO}_2$ , 33.12% of  $\text{Al}_2\text{O}_3$  and 13.09% of MgO. The X-ray diffraction analysis showed that cordierite ceramics was formed but the intensity of the peaks was not very high which indicates the presence of

amorphous phases. Increasing MgO content and decreasing Al<sub>2</sub>O<sub>3</sub> content did not significantly affect the phases obtained. The thermal analysis result indicates the loss of surface water between 100 and 200 °C as well as the chemically-bonded water between 300 °C and 480 °C and a region of stability between 480 °C, and 900 °C. As the amount of MgO increases with decreasing Al<sub>2</sub>O<sub>3</sub> content, the intensity of the endothermic peak decreases. The morphology of the samples indicates that as the amount of MgO increases, the average size of the grains decreases, the level of grain inhomogeneity also decreases. The highest density value was obtained with sample A i.e. the correct composition of the cordierite. Increasing the content of MgO led to a reduction in the density values. There was also no significant trend observed.

## 5. ACKNOWLEDGMENT

The authors wish to acknowledge the assistance and contributions of the laboratory staff of the Department of Metallurgical and Materials Engineering, Faculty of Engineering, University of Lagos, Akoka, Lagos state toward the success of this work.

## 6. CONFLICT OF INTEREST

There is no conflict of interest associated with this work.

## REFERENCES

- Albhillil, A.A., Palou, M., Kozankova, J. and Slovaca, A. C. (2013). Characterization of cordierite-mullite ceramics prepared from natural raw materials. *Slovak University of Technology (STU) Bratislava*. 6(1), pp. 1-7
- Cao, J., Shi, X., Zhang, C., Li, Z., Luo, N. and Cui, H. (2016). A study of synthesis of cordierite powder. 6<sup>th</sup> international conference on Mechatronics, Materials, Biotechnology and Environment. *Atlantis Press China*, pp. 344-350.
- Croitoru L., Chang C. J. and [Akpokodje J.](#) (2020). The Health Cost of Ambient Air Pollution in Lagos. [Journal of Environmental Protection](#), 11(9), pp. 753-765
- El-Buaishi, M. N., Jankovic-Castvan I., Jokic B., Veljovic D., Janackovic D. and Petrovic, R. (2012). Crystallization behaviour and sintering of cordierite synthesized by aqueous sol-gel route. *Ceramics International*, 38(3), pp. 1835-1841.
- Eing, K. K., Johar, B., Ho, L. N. and Zabar, Y. (2016). Influence of sintering temperature on crystallization behaviour of cordierite synthesized from the non-stoichiometric formulation. *MATEC Web of Conferences* 78, 01099
- Gokce, H., Ovecoglu, M., Aslanoglu, Z. and Ozkal, B. (2004). Microstructural characterization of cordierite ceramics produced from natural raw materials and synthetic powders. *Key Engineering Materials*, 264- 268, pp. 1035-1038.
- Gonzalez – Velasco, J.R., Gutierrez – Ortiz, M.A., Ferret, R., Aranzabal, A. and Botas. J.A. (1999). Synthesis of cordierite monolithic honeycomb by solid-state reaction of precursor oxides. *Journal of Materials Science*, 34, pp. 1999-2002.
- Gunay, E. (2010). Sintering behavior and Properties of sepiolite-based cordierite composition with added boron oxide. Tubitak-MRC, Materials Institute, Turkey, pp. 83-92.
- Jianfeng, W., Chenglong, L., Yaxiang, X. Z., Dongbin, W. and Qiankun, Z. (2018). Cordierite Ceramics prepared from Poor Quality Kaolin for Electric Heater Supports. *Journal of Wuhan University of Technology*, 33(3), pp. 598–607.
- Khabas, T. A., Vereshchagin, V. I., Vakalova, T. V., Kirchanov, A. A., Kulikovskaya, N. A. and Kozhevnikova, N. G. (2003). Low-Temperature synthesis of the Cordierite phase in ceramic Mixtures of Natural Raw Materials. *Journal of Refractories and Industrial Ceramics*, 44, pp. 181-185.
- Mai, P. P., Tien, N. T., Minh, T. L. and Driessche, I. V. (2015). The application of high surface area cordierite synthesized from kaolin as a substrate for auto exhaust catalysts. *Journal of the Chinese chemical society*, 62, pp. 536–546.

Naskar, M. K. and Chatterjee, M. (2004). A novel process for the synthesis of cordierite ( $Mg_2Al_4Si_5O_{18}$ ) powders from rice husk and other sources of silica by sol-gel technique. *Journal of the European Ceramic Society*, 24, pp. 3499-3508.

Ning, W., NTang, Z., Han, Z., Ding, S., Xu, C. and Zhang, P. (2018). Studied the effect of  $NH_4VO_3$  on properties and structures of Cordierite Ceramics. *Journal of Ceramic Science and Technology*, 9, pp. 47-52.

Sumi, K., Kobayashi, Y. and Kato, E. (2004). Low-Temperature Fabrication of Cordierite Ceramics from Kaolinite and Magnesium Hydroxide Mixtures with Boron Oxide Additions. *Journal of America Ceramic Society*, 82, pp. 783-785.

Zhu, P., Wang, L.Y., Hong, D. and Zhou, M. (2012). A Study of cordierite ceramic synthesis from serpentine Tailings and Kaolin Tailing. *Science of Sintering*, 44, pp. 129-134.